

### 13. STRUCTURAL ANALYSIS OF PLAGIOCLASE-BEARING PERIDOTITES EMPLACED AT THE END OF CONTINENTAL RIFTING: HOLE 637A, ODP LEG 103 ON THE GALICIA MARGIN<sup>1</sup>

Jacques Girardeau, Laboratoire de Pétrologie Physique, Institut de Physique du Globe de Paris et Université Paris VII, Paris, France

Cynthia A. Evans,<sup>2</sup> Lamont-Doherty Geological Observatory, Palisades, New York  
and

Marie-Odile Beslier, Laboratoire de Pétrologie Physique, Institut de Physique du Globe de Paris et Université Paris VII, Paris, France

#### ABSTRACT

A ridge of peridotite, 100 km long and a few kilometers wide, borders the western edge of the Galicia passive continental margin (Spain) at the contact with oceanic crust. This ridge was drilled at Hole 637A during ODP Leg 103. The peridotites are serpentinized diopside-rich spinel- or spinel + plagioclase-bearing harzburgites and lherzolites that underwent only limited melt extraction during their ascent within the lithosphere.

The foliation in the peridotites shows a nearly constant attitude; dip is constant (20°–30°) to the east-northeast in the upper 50 m of the section and increases to 70° in the deepest 20 m. The stretching lineation is generally downdip (i.e., nearly east-west) except locally, where it is at 45° to the downdip direction. The peridotite, initially coarse grained, displays a mylonitic disrupted texture. It has been plastically deformed in a rotational regime (simple shear), under high-stress conditions (~180 MPa), at high but decreasing temperatures (from up to 1000° to 850°C), and probably at very shallow depths (<7 km). High strain intensities ( $\gamma = 12$ ) are estimated for the mylonite formation. After ductile shearing, the peridotite underwent some brittle deformation, allowing for complete serpentinization and the opening of fractures that are now filled by serpentine and calcite. Some fracturing continued after the calcite injection.

The Hole 637A peridotites probably represent asthenospheric material emplaced in a stretched continental margin during the first stage of ocean accretion. The geometry and kinematics of the peridotite emplacement are consistent with a roughly east-west opening of the Atlantic Ocean.

#### INTRODUCTION

From samples recovered by dredging and drilling in oceanic domains, it is now known that the oceanic floor is not always made of mafic rocks but also consists locally of serpentinized peridotites. These peridotites comprise escarpments or protrusions in transform faults (Bonatti and Honnorez, 1976; Bonatti and Hamlyn, 1978; 1981) and blocks forming topographic highs along oceanic ridges (Mid-Atlantic Ridge; Aumento and Loubat, 1971; Tiezzi and Scott, 1980) or are intercalated within sediments or basalts (Mid-Atlantic Ridge, DSDP Leg 37—Helmstaedt, 1977; Sigurdsson, 1977; DSDP Leg 45—Boudier, 1979; Sinton, 1979; DSDP Leg 82—Michael and Bonatti, 1985; ODP Leg 109—Bryan et al., 1986). Peridotites also crop out on the ocean floor of some incipient oceans (Red Sea—Bonatti et al., 1981, 1986; Styles and Gerdes, 1983; Nicolas et al., 1985, 1987) or small oceans (Tyrrhenian Sea—Kastens et al., 1986), and they locally form elongate ridges at the boundary between continental and oceanic domains (southwest of Australia—Nicholls et al., 1981; northwestern part of the Iberian margin—Boillot et al., 1980, 1986a). Similar occurrences are documented in ancient rocks, as shown by studies of remnants of oceanic floor such as the Western Alps ophiolites (Decandia and Elter, 1982; Lombardo and Pognante, 1982; Lagabriele, 1982; Lemoine et al., 1987).

Explanations for the presence of peridotites on or close to the seafloor are still debated. These occurrences can result from secondary tectonics (fault displacement) or from primary man-

tle upwelling processes. In places where the oceanic crust is very thin, such as along transform faults or along ridge valleys of slow-spreading ridges, it is quite possible that the peridotites were carried directly onto the oceanic floor by motion along normal faults. Such a mechanism has been proposed to explain the uplift of the peridotites recovered along ridges or transform-fault segments of ridges. However, this does not explain the original ascent of peridotites exposed on Zabargad Island (Nicolas et al., 1985, 1987; Bonatti et al., 1986), in the Alps (Nicolas, 1984), in the Betics (Obata, 1977; Tubia and Cuevas, 1987), and in the Pyrenees (Vielzeuf and Kornprobst, 1984; Kornprobst and Vielzeuf, 1984) in consideration of their petrological and structural characteristics; these peridotites probably resulted from hot mantle uplift during continental rifting or transcurrent crustal thinning. Finally, to explain the peridotites cropping out at the boundary between continents and oceans, Boillot et al. (1986b, 1987) proposed that the rise of peridotites to the surface can result simply from tectonic denudation of the mantle as a consequence of stretching of the lithosphere during rifting.

The peridotites cropping out along the oceanic crust at the foot of the Galicia margin (northwestern Spain) were cored at Hole 637A during Ocean Drilling Program (ODP) Leg 103. This paper presents a structural study of these peridotites aimed at defining their deformation history. From the geometry of the peridotite ridge, the kinematics of emplacement of the peridotites, and the physical conditions prevailing during their uplift as inferred from microstructural and petrological data, we attempt to constrain mantle-rising processes during the first stages of ocean formation.

#### REGIONAL BACKGROUND

The Galicia margin is a deep, 300-km-wide passive continental margin extending west from the Iberian Peninsula (Fig. 1).

<sup>1</sup> Boillot, G., Winterer, E. L., et al., 1988. *Proc. ODP, Sci. Results*, 103: College Station, TX (Ocean Drilling Program).

<sup>2</sup> Present address: CA8, NASA, Johnson Space Center, Houston, TX 77058.

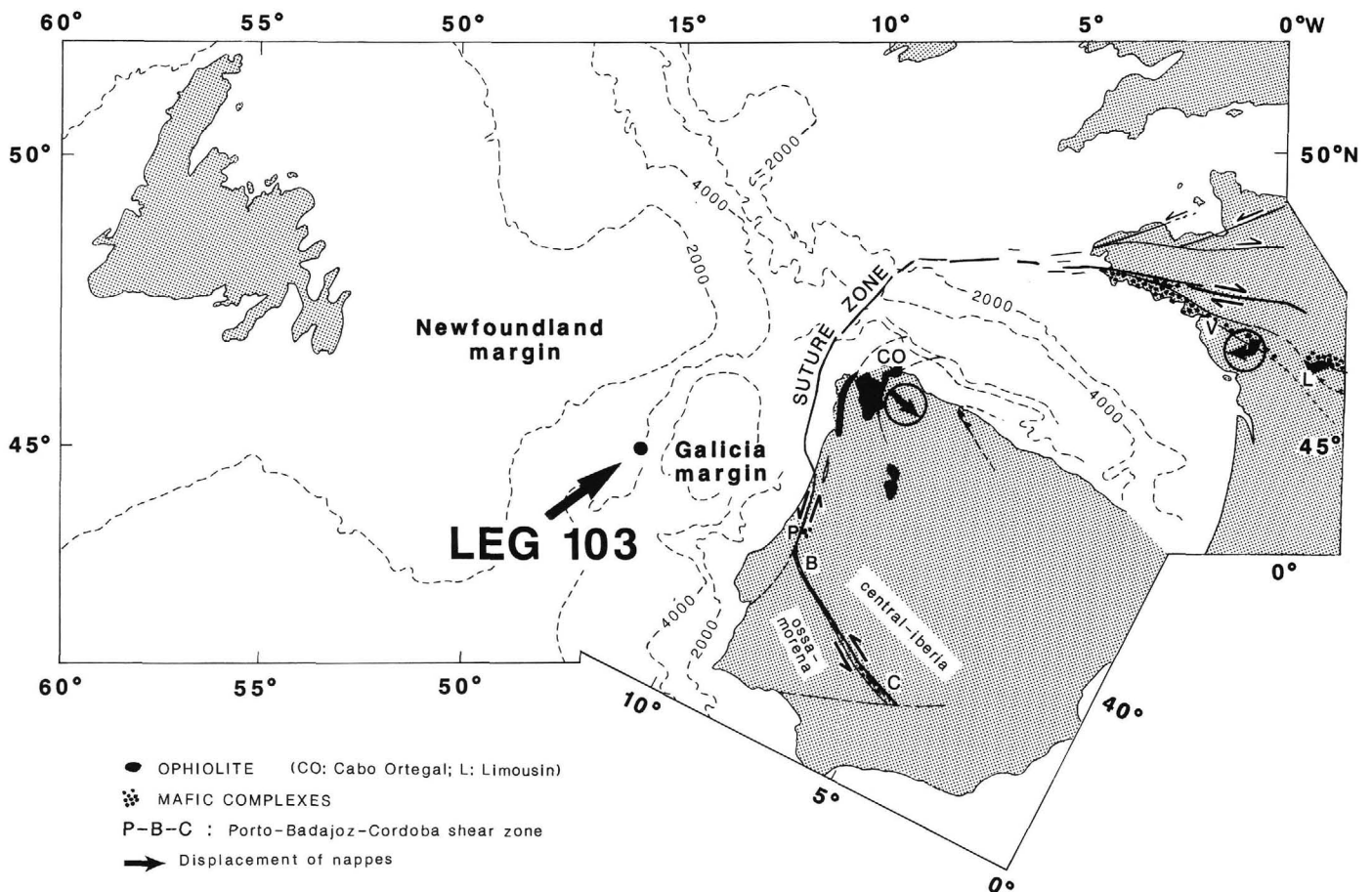


Figure 1. Sketch map showing the continent pattern before the North Atlantic opening (modified after Lefort, 1980; Lefort and Ribeiro, 1980; Burg et al., 1981). The circled arrows give the sense of displacement of the nappes; CO = Cabo Ortégal (data from Iglesias et al., 1983; Matte, 1983; 1986); V = Vendée and L = Limousin (Burg, 1981; Brun and Burg, 1982; Girardeau et al., 1986; Burg et al., 1987).

The lithology of the Galicia margin plutonic and metamorphic basement from dredge data indicates that the Galicia margin belongs to the Ossa-Morena Zone, rather than the Central Iberia Zone (Capdevila and Mougénot, this volume). The Galicia margin is separated from the central part of Iberia by a major tectonic discontinuity (Lefort, 1980; Lefort and Ribeiro, 1980) corresponding to the northern extension of the Porto-Badajoz-Cordoba sinistral shear zone (Burg et al., 1981), which represents the major Variscan suture zone (Fig. 1). Kinematics of the Variscan collision zone imply a top-to-the-southeast shear during nappe emplacement in Galicia area (Iglesias et al., 1983; Matte, 1983, 1986) making interpretation of Hole 637A peridotites as remnants of a Variscan sheet difficult. Petrologic and structural comparison between the Hole 637A peridotites and the Variscan peridotites (Cabo Ortégal—Vögel, 1967; Van Calsteren, 1978; Iburguchi et al., 1987) (Limousin—Dubuisson et al., 1987) supports this, and we will not further consider the Variscan nappe hypothesis in this paper.

The Galicia margin is made up of several blocks that are well defined on Sea Beam bathymetric maps (Sibuet et al., 1987) and on seismic profiles (Montadert et al., 1974, 1979; Groupe Galice, 1979) (Figs. 2A and 2B). The blocks are tilted to the east (Fig. 2B) and the resulting half-grabens are filled by Lower Cretaceous syn-rift sediments and disconformably covered by a post-upper Aptian post-rift sedimentary sequence (Sibuet and Ryan, 1979). The southern part of the margin was not affected by the Pyrenean tectonics, unlike its northern part, which was gently tilted and uplifted (Boillot et al., 1979).

A 100-km-long, 10-km-wide ridge of peridotites borders the western part of the margin along the Iberian Abyssal Plain. Geophysical data suggest that this abyssal plain is underlain by typical oceanic crust. The ridge, generally buried under Mesozoic and Cenozoic sediments, crops out on Hill 5100 in the southwestern part of the margin, and resembles a dome or a tilted block on seismic profiles (Figs. 2C and 2D). Petrologic study of a strongly weathered sample recovered by dredging revealed that the ridge is composed of totally serpentized spinel-plagioclase-bearing lherzolite showing subcontinental affinities (Boillot et al., 1980). These authors proposed that the ridge was made of totally serpentized peridotites emplaced by diapirism (buoyancy) during the first stages of formation of the Atlantic Ocean.

## HOLE 637A PERIDOTITES

### Petrographic Data

Seventy meters of peridotites was cored on the eastern flank of Hill 5100 at Hole 637A (Cores 103-637A-23R through 103-637A-30R), but only 39 m of rock was recovered, consisting of yellow to brown peridotites that generally display a well-defined foliation (Fig. 3A). The section is locally crosscut by mylonitic shear zones (Fig. 3B) except at the top (Core 103-637A-23R and part of Core 103-637A-24R), where they are almost totally replaced by calcite, and the base (parts of Cores 103-637A-28R and 103-637A-29R), where they are strongly brecciated and crosscut by abundant calcite or serpentinite veins. Calcite veins are

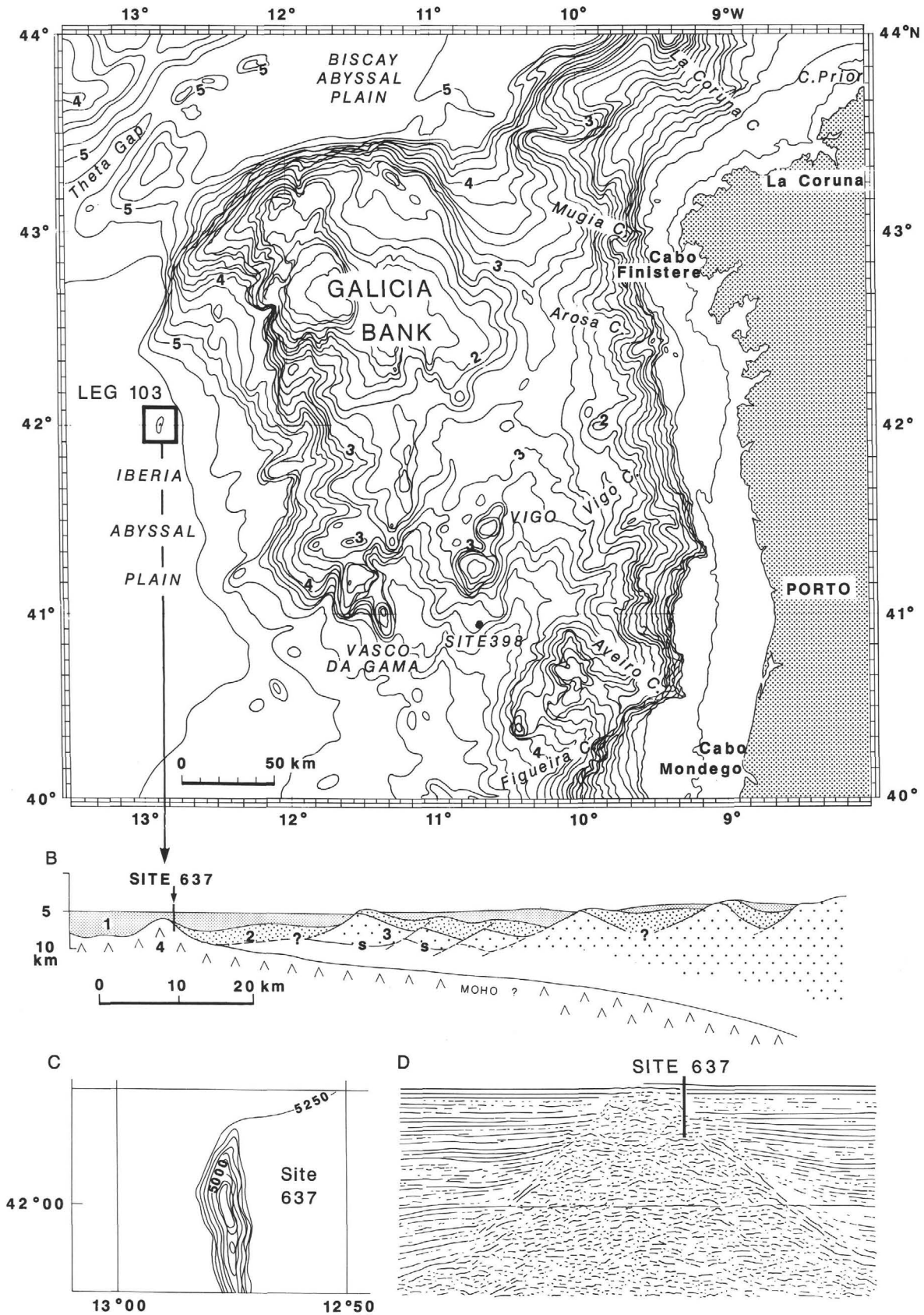


Figure 2. Location of Hole 637A at the boundary between the stretched continental margin (Galicia margin) and the Iberian Abyssal Plain on Hill 5100. A. Bathymetry after Lallemand et al. (1986). B. Interpreted cross section from Boillot et al. (1986a). C. Sea Beam bathymetry from Sibuet et al. (1979). D. Seismic profile from Institut Français du Pétrole (courtesy of L. Montadert).

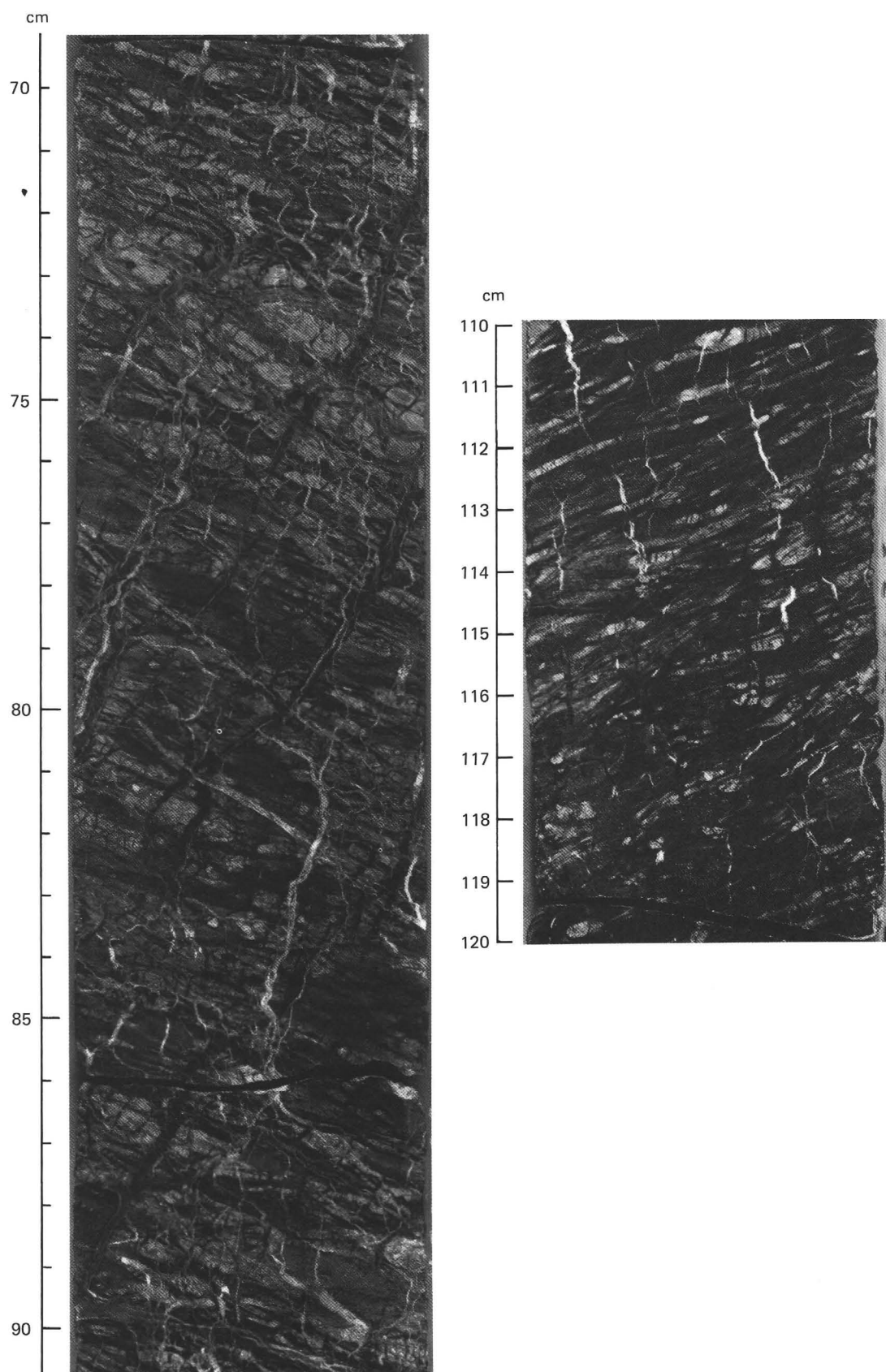


Figure 3. Core photographs. **A.** Representative texture of the Hole 637A peridotites (Sample 103-637A-26R-2, 69-91 cm). The peridotite is rich in orthopyroxene, with a well-developed foliation plane roughly corresponding to the  $S_1$  mylonitic foliation. **B.** Five-cm-thick shear zone crosscutting the  $S_1$  foliation (Sample 103-637A-25R-4, 110-120 cm). Note that the peridotite becomes less depleted in orthopyroxene downsection.

common throughout the cored section (Samples 103-637A-23R-2, 135–150 cm, 103-637A-23R-3, 0–100 cm, 103-637A-24R-1, 0–150 cm, 103-637A-25R-1, 0–150 cm, 103-637A-25R-2, 0–150 cm, 103-637A-25R-3, 0–105 cm, 103-637A-25R-4, 20–100 cm, 103-637A-25R-5, 0–150 cm, 103-637A-25R-6, 0–80 cm, 103-637A-26R-1, 1–40 cm, 103-637A-26R-3, 0–150 cm, 103-637A-26R-4, 0–60 cm, 103-637A-27R-1, 1–105 cm, 103-637A-27R-2, 1–110 cm, 103-637A-27R-3, 1–50 cm, 103-637A-27R-4, 1–105 cm, 103-637A-27R-5, 0–105 cm, 103-637A-27R-6, 1–105 cm, 103-637A-28R-1, 30–150 cm, and 103-637A-28R-2, 40–150 cm) and probably correspond to minor (centimeter- to meter-thick), late brittle faults of unknown geometry.

Although the peridotites are generally strongly serpentinized or replaced by calcite, most of the more than 70 samples studied contain fresh relicts of the primary phases, that is, olivine, spinel, orthopyroxene, clinopyroxene, and some plagioclase. The original modal composition of the peridotite would have varied mostly from diopside-rich harzburgites (diopside  $\approx$  2%) to lherzolites (diopside = 5%–7%). However, more depleted facies occur in some places (Samples 103-637A-25R-4, 125–150 cm, 103-637A-26R-4, 60–75 cm, 103-637A-27R-1, 110–150 cm, and 103-637A-28R-2, 1–40 cm). The peridotites also display locally some orthopyroxene-rich facies (Samples 103-637A-25R-5, 17–30 cm, 103-637A-25R-6, 89–91 cm, 103-637A-26R-1, 128–150 cm, and 103-637A-27R-4, 60–65 cm) and, more rarely, thin clinopyroxene lenses, about 5 mm thick and a few centimeters long (Samples 103-637A-25R-1, 100–102 cm and 103-637A-26R-3, 29–30 cm). Although fresh clinopyroxene and spinel occur in almost all of the samples studied, only a few still contain olivine relicts. Plagioclase is rarely fresh and is, therefore, difficult to recognize; it rims spinel, constitutes isolated interstitial crystals (Fig. 4A), or forms discontinuous veinlets (Fig. 4B). Secondary products, including various types of amphiboles and serpentines, chlorite, magnetite, hematite, and clay minerals, have developed in the peridotites to various degrees in the presence of water (Agrinier et al., this volume). Despite the pervasive alteration of the rocks, the shapes of some of the primary phases (in particular that of orthopyroxene), are recognizable in thin sections or on polished samples.

### Structural and Microstructural Data

#### Previous Data

The main tectonic structures observed in the Hole 637A peridotites, foliation planes of the peridotites and injection planes

of the calcite veins, were directly measured aboard ship. The former structures have been related to high-temperature plastic deformation and the latter to brittle deformation that would have occurred after the peridotite was serpentinized (i.e., probably after the peridotite was in its present tectonic position). From our shipboard study, we concluded that the main foliation plane (Fig. 5) in the peridotite dips about 20°–30° in the upper 50 m of the cored section (Cores 103-637A-23R through 103-637A-28R), increasing to 70° in the bottom 20 m of the section (Cores 103-637A-28R and 103-637A-29R). According to the paleomagnetic data (see “Site 637” chapter; Shipboard Scientific Party, 1987), the foliation dips to the east; this interpretation was later confirmed by diving with the submersible *Nautilie* on the western flank of Hill 5100 (Boillot et al., 1986a; this volume). The lineation is oriented downdip in the foliation (i.e., east-west), and shear sense indicates a top-to-the-east motion along the shear planes. The calcite veins were injected in planes parallel to the foliation or in planes perpendicular to both foliation and lineation in the peridotite. Their attitudes are consistent with normal displacement along late faults parallel to the peridotite foliation. This paper does not give any new structural data about the calcite vein injection, which occurred at very low temperature when the peridotite was close to the seafloor (Agrinier et al., this volume; Kimball and Evans, this volume; Evans and Baltuck, this volume). Note, however, that some fracturing of the peridotite postdates injection of the calcite veins.

#### New Data

Structural analysis of the peridotites presented in this paper was performed on about 70 samples. All of these samples were cut parallel to the foliation plane to measure the stretching lineation, which was not identified aboard ship. Thin sections were cut parallel to the *XZ* and *YZ* planes for strain-stress analysis.

Shore-based analysis of the general attitude of the foliation agrees with that determined aboard ship (Fig. 5). This foliation roughly corresponds to the  $S_1$  mylonitic foliation obvious throughout the recovered section (Figs. 3A and 6A). However, deformation is heterogeneous, as is best evidenced in the freshest samples (Samples 103-637A-27R-3, 31–33 cm, and 103-637A-27R-3, 46–48 cm), which exhibit several types of textures that allow for understanding of the evolution of the peridotite.

A “primary”  $S_0$  foliation can be recognized in the peridotites, marked by spinel crystals (Fig. 6B). The  $S_0$  foliation is cross-

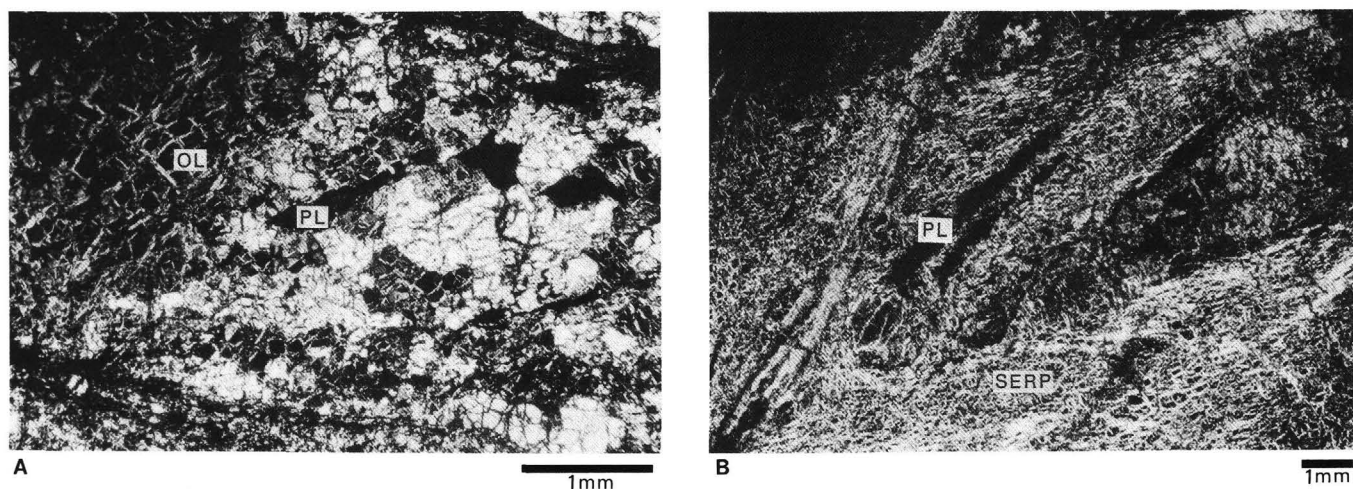


Figure 4. Photomicrographs of thin sections showing plagioclase (PL) forming (A) interstitial crystals (Sample 103-637A-27R-3, 46–66 cm) or (B) veinlets (Sample 103-637A-27R-2, 114–117 cm). OL = olivine; SERP = serpentine.

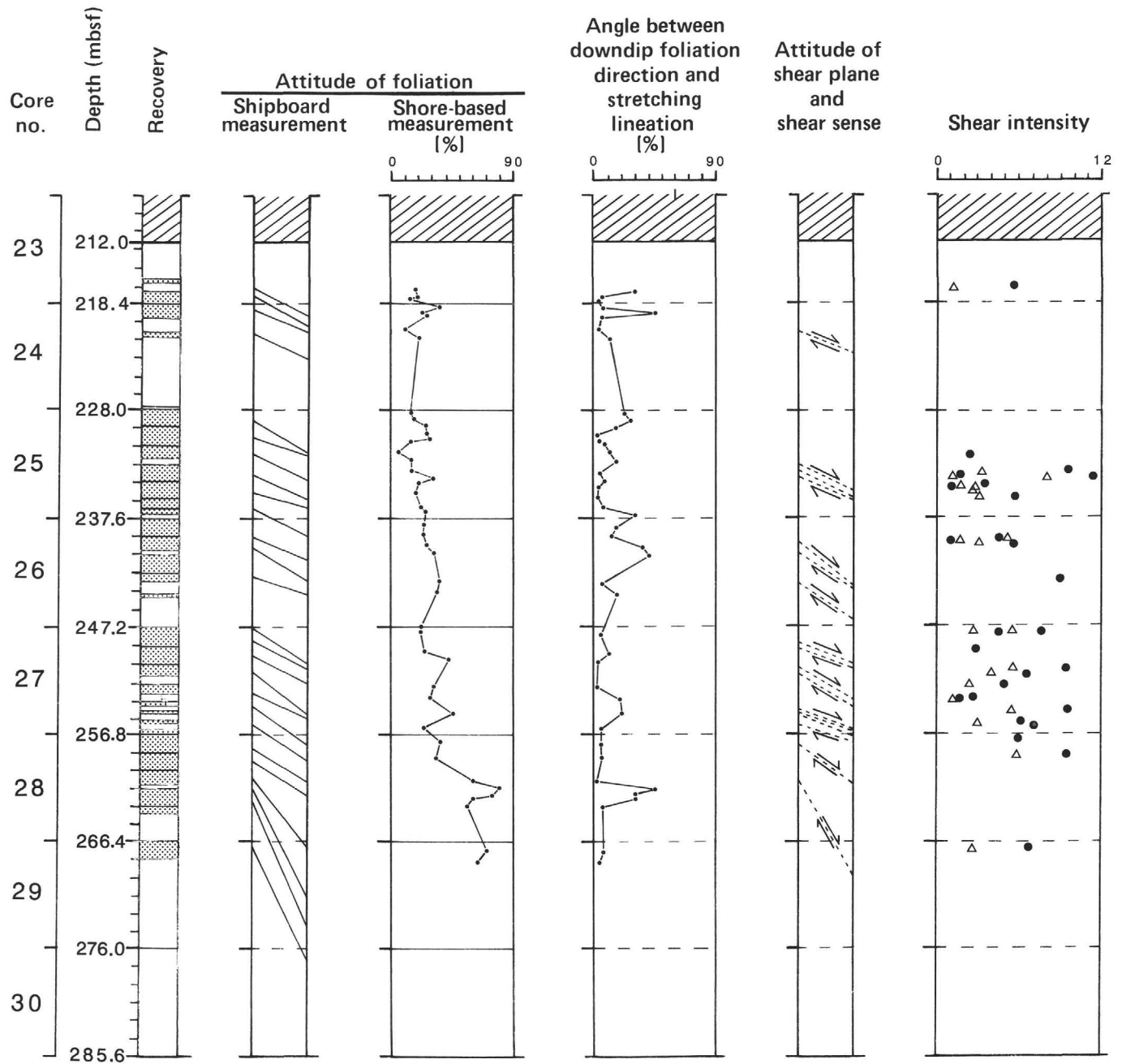


Figure 5. Schematic structural and microstructural cross sections of peridotite recovered at Hole 637A. Shear intensity (far right column) determined using the formula  $\gamma = 2\cot\theta\alpha$  (solid circles) and  $\gamma = \lambda_1 - \lambda_2$  (open triangles).

cut at a small angle ( $15^\circ$  to  $30^\circ$ ) by an  $S_1$  mylonitic foliation that is well defined by highly stretched orthopyroxene crystals (Figs. 6A–6D). When present, the olivine porphyroclasts (which are poorly recrystallized at their periphery into large neoblasts) are elongate parallel to this  $S_1$  foliation, displaying wide kink bands (Figs. 6C and 6D). Along the mylonitic bands, all primary phases, such as pyroxenes (both orthopyroxene and clinopyroxene), olivine, and spinel, have recrystallized into a fine-grained matrix (Fig. 6E). The thickness of these mylonitic bands varies from a few millimeters to more than 10 cm. One of the most important characters of these mylonites is the existence of thin (generally less than 1 mm thick) ultramylonitic bands that cross-cut the whole rock (Figs. 6C and 6D). In these bands there is a drastic grain-size reduction with respect to that observed in the

mylonitic foliation (Fig. 6E). The ultramylonitic bands produce some boudinage of the orthopyroxene crystals and lead to the formation of a disrupted texture in most of the peridotites studied. Where olivine no longer exists, the mylonitic foliation and the ultramylonitic bands can still be recognized (Fig. 6A). On the other hand, the  $S_0$  foliation,  $S_1$  mylonitic foliation, and ultramylonitic bands dip the same direction, with  $S_1$  being steeper than  $S_0$  and the ultramylonitic bands steeper than  $S_1$ . The rotation of these successive structures is consistent with that expected from the shear sense determined from these rocks (see the following sections).

Plagioclase has recrystallized together with the other primary phases along the ultramylonitic bands. It generally rims spinel, concentrates in bands parallel or oblique to the  $S_1$  foliation, or

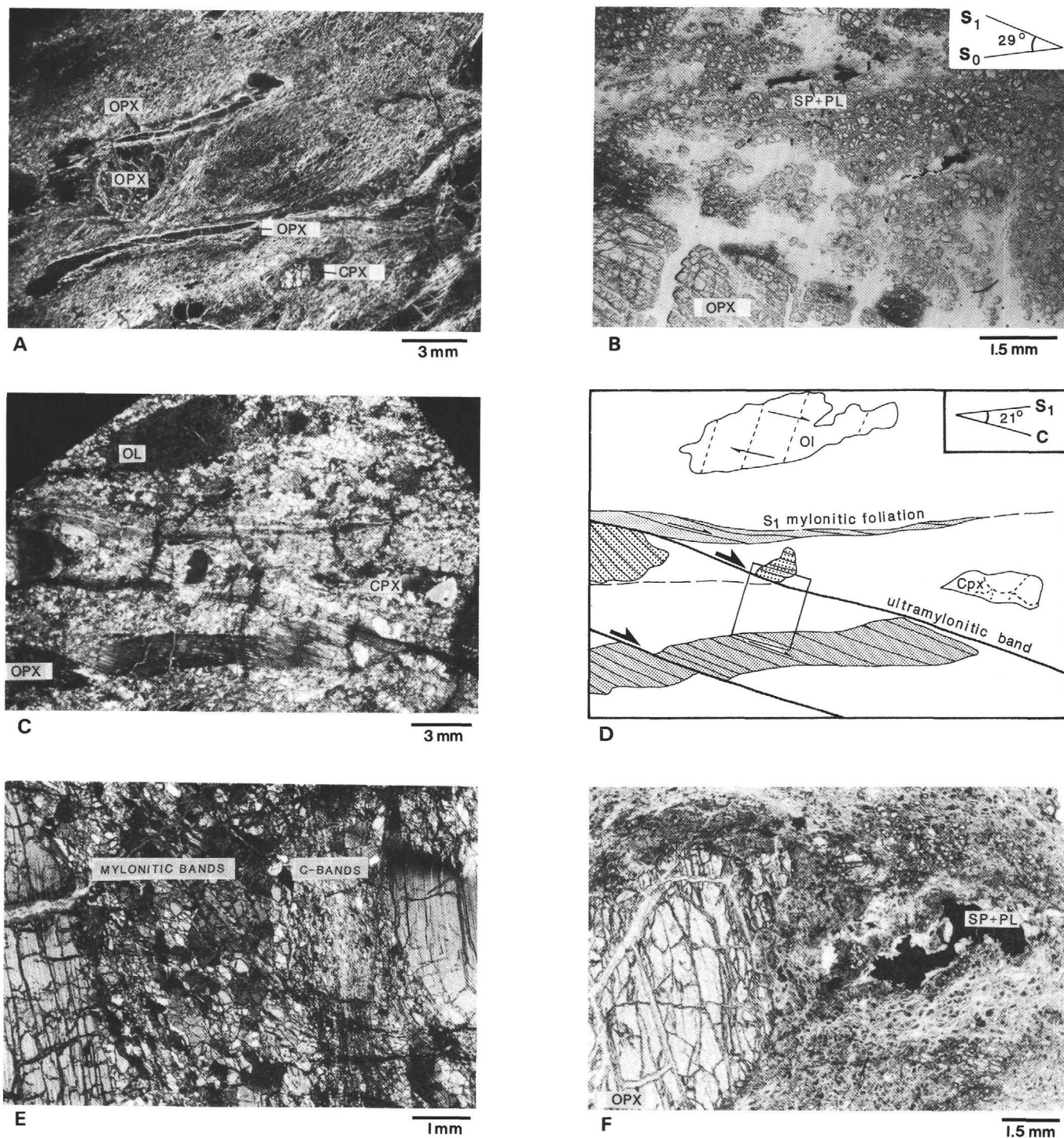


Figure 6. Photomicrographs of thin sections showing representative textures of the Hole 637A peridotites. **A.** Totally serpentinized peridotite. The extremely elongated orthopyroxene (OPX) crystals (now completely transformed into bastite) that define the  $S_1$  mylonitic foliation coexist with rounded ones. Clinopyroxene (CPX) has completely recrystallized and locally forms asymmetric lenses. This heterogeneous disrupted texture is the most common texture of the Hole 637A peridotites (Sample 103-637A-28R-2, 2–25 cm). **B.** Attitude of  $S_0$  foliation marked by elongate spinels (black) relative to the  $S_1$  mylonitic foliation defined by the orthopyroxene crystal (OPX) elongation. Note that spinel is rimmed by plagioclase (white) (Sample 103-637A-27R-3, 31–33 cm). **C and D.** Attitude of the  $S_1$  mylonitic foliation marked by strongly elongated orthopyroxene crystals (dashed crystals) relative to the ultramylonitic bands along which the grain size is extremely reduced. Note the presence of large olivine porphyroclasts remnants (OL) and of totally recrystallized clinopyroxene (CPX) lenses. The ultramylonitic bands crosscut the  $S_1$  foliation at about  $20^\circ$ , producing some boudinage of the orthopyroxene crystals. Displacement along the ultramylonitic bands sometimes reaches 1 cm (Sample 103-637A-27R-3, 31–33 cm). **E.** Reduction in grain size from the  $S_1$  mylonitic foliation to the ultramylonitic C-band (Sample 103-637A-27R-3, 31–33 cm). **F.** Spinel (black) asymmetric crystallization queue developing from a rounded asymmetric orthopyroxene crystal (OPX). Note that spinel is rimmed by plagioclase (white) (Sample 103-637A-23R-3, 44–46 cm).

forms interstitial crystals that may have crystallized from trapped magmas (Fig. 4A). More rarely, the plagioclase constitutes crystallization aggregates of asymmetrical, subspherical orthopyroxene crystals (Fig. 6F), which may suggest that plagioclase formed partly during the  $S_1$  deformation. However, these structures might simply reflect some migration of plagioclase during deformation.

The stretching lineation is generally subparallel to the foliation down-dip direction. However, it sometimes stands at about  $45^\circ$  from the foliation, particularly in samples for which the foliation dips sharply (Fig. 5), as is also the case to the north of the studied area (Beslier et al., 1988).

### Physical Conditions of Deformation

#### *Regime of Deformation and Shear Sense*

The noncoaxial regime of the deformation is evidenced at different scales, principally by the development of the ultramytonitic bands interpreted as shear bands (Figs. 6C and 6D) or the  $\alpha$  obliquity on petrofabric diagrams (Fig. 7), but also by the asymmetry of the pyroxene crystals and subsequent crystallization aggregates (Fig. 6F). Figures 6C and 6D show that the olivine glide plane (perpendicular to the kink band boundaries), the orthopyroxene glide planes (parallel to the exsolution lamellae), and the ultramytonitic bands are all parallel, indicating that they formed during the same deformation event. Four representative olivine- and orthopyroxene-porphroclast-petrofabric diagrams are shown in Figure 7. Olivine displays good crystallographic orientations (Figs. 7A and 7C), with the [010] axes oriented at a high angle to the foliation and the [100] axes close to the spinel lineation. Such a fabric indicates that the deformation occurred in a noncoaxial regime by translation glide according to the [100] (010) slip system, which is activated at high temperature ( $\geq 1000^\circ\text{C}$  for geological strain rates, that is,  $\approx 10^{14}/\text{s}$ ; Carter and Avé Lallemant, 1970; Mercier, 1986). The orthopyroxenes (Figs. 7B and 7D) also show a good preferred orientation in agreement with the (100) [001] slip system activated at high temperature. Following Mercier (1986) and in consideration of the deviatoric stress values estimated here for mylonitization of the peridotite ( $\approx 180$  MPa; see next section), the (010) [100]/{0kl}[100] olivine glide-system transition curve attitude, and also that of the enstatite slip-twinning inversion, we can estimate that the deformation responsible for the formation of the  $S_1$  foliation occurred at a minimum temperature of  $1000^\circ\text{C}$ .

The absence of double maxima or conjugate girdles of  $[010]_{\text{ol}}$  and  $[100]_{\text{en}}$  (projections of the glide planes) on the petrofabric diagrams strongly suggests that deformation occurred dominantly by simple shear or that the pure shear component was negligible. The constant attitude of the orthopyroxene slip planes with respect to the foliation in all study samples is consistent with such a hypothesis.

The shear sense can be best determined on petrofabric diagrams using the angle  $\alpha$  between the foliation and shear planes. The shear sense can also be determined using the obliquity between the elongation plane of the orthopyroxenes and their (100) exsolution glide planes. Single-crystal shear senses are all consistent and therefore, are regarded as reflecting the general sense of shear of the rocks. Regardless of which of the three methods is used, all measurements give the same sense of shear (Fig. 5).

#### *Strain Intensity*

The strain intensity,  $\gamma$ , can be estimated using the formula  $\gamma = 2\cot\theta 2\alpha$  (Nicolas and Poirier, 1976). The obliquity,  $\alpha$ , is the angle between the foliation plane and the shear plane and can be measured on olivine fabrics or directly estimated on thin sections in which orthopyroxenes present a strong elongation, with

the shear plane being parallel to the (100) clinopyroxene exsolution lamellae. The  $\alpha$  obliquity ranges from  $10^\circ$  to  $20^\circ$ , yielding  $\gamma$  values ranging from 2.3 in the least deformed facies to 11.6 in the true mylonites (Fig. 8A).

The strain intensity can also be estimated using the formula  $\gamma = \lambda_1 - \lambda_2$  (Ramsay, 1967), assuming that deformation occurred by simple shear. It is possible to reconstruct the initial shapes of the stretched orthopyroxene crystals because their elongation results from gliding along the (100) slip planes marked by the exsolution lamellae. This allows direct estimation of  $\lambda$  by using the formula  $\lambda = 1 + e$ , where  $e = (l_1 - l_0)/l_0$  and  $l_0$  and  $l_1$  represent the initial and final lengths of the crystal, respectively. The  $\lambda$  values obtained by this method vary from 0.2 to 8.2. (Fig. 8B).

Reconstructed orthopyroxene crystals sometimes have typical rectangular or rounded shapes. However, many of them have their (100) slip plane perpendicular to their elongation (as those defining the "b" lineations of Darot and Boudier, 1975). This implies that these orthopyroxene crystals derive from what were once much larger crystals that were disrupted along subgrain boundaries during an earlier deformation possibly related to the formation of the  $S_0$  foliation. Therefore, we consider that the initial peridotite had a very coarse grain characterized by the presence of large orthopyroxene crystals. The latter feature, however, could come from previously existing orthopyroxene-rich bands, now strongly boudinaged and scattered within the peridotite.

The  $\gamma$  strain intensities obtained by these two methods largely underestimate the bulk deformation encountered by the peridotite, because most of the stretching of the rock occurred by plastic gliding of the olivine matrix, which is much less competent. The average stretching amount calculated from the pyroxene elongation is about 280% for the whole section, with a maximum value of 730%.

#### *Stress Estimates*

The deviatoric stress  $\sigma_D = \sigma_1 - \sigma_3$  can be directly estimated from the olivine recrystallized grain size, according to experimental data (Post, 1973; Mercier et al., 1977; Ross et al., 1980). Depending on the recrystallization process, two distinct laws have been established for stress estimates:

$$\begin{aligned}\sigma_D &= 74.5D^{-1} \text{ for subgrain rotation (SGR) (Mercier, 1980)} \\ \sigma_D &= 4.81D^{0.787} \text{ for grain-boundary migration (GBM) (Ross et} \\ &\text{al., 1980),}\end{aligned}$$

where the deviatoric stress is in MPa, and  $D$  represents olivine grain size measured in millimeters.

Although the peridotites are generally strongly serpentized, some samples contain abundant olivine remnants (Samples 103-637A-27R-3, 31-33 cm, and 103-637A-27R-3, 46-50 cm). They display well-developed disrupted textures with several generations of neoblasts growing from preexisting porphyroclasts (Fig. 6C). The latter are rather scarce, but a few of them persist in the peridotites. They are only poorly recrystallized into large, poorly oriented neoblasts ( $\approx 1$  mm); thus, it is possible to define their initial shapes and thereby estimate their minimum sizes. The larger crystals are 10 mm long (Figs. 6C, 6D, and 9), which evidences a low-stress (0.7 to 7 MPa) deformation history before the development of the  $S_1$  mylonitic foliation and ultramytonitic bands. Intensive recrystallization occurred during the formation of the  $S_1$  mylonitic foliation, along which the neoblast grain size averages 0.3 mm (Figs. 6E and 9), which leads to  $\sigma_D$  stress estimates of about 190 MPa. In the ultramytonitic bands, the neoblast grain size is extremely reduced to only 0.01 mm on average (Figs. 6E and 9), which also yields very high stress values for

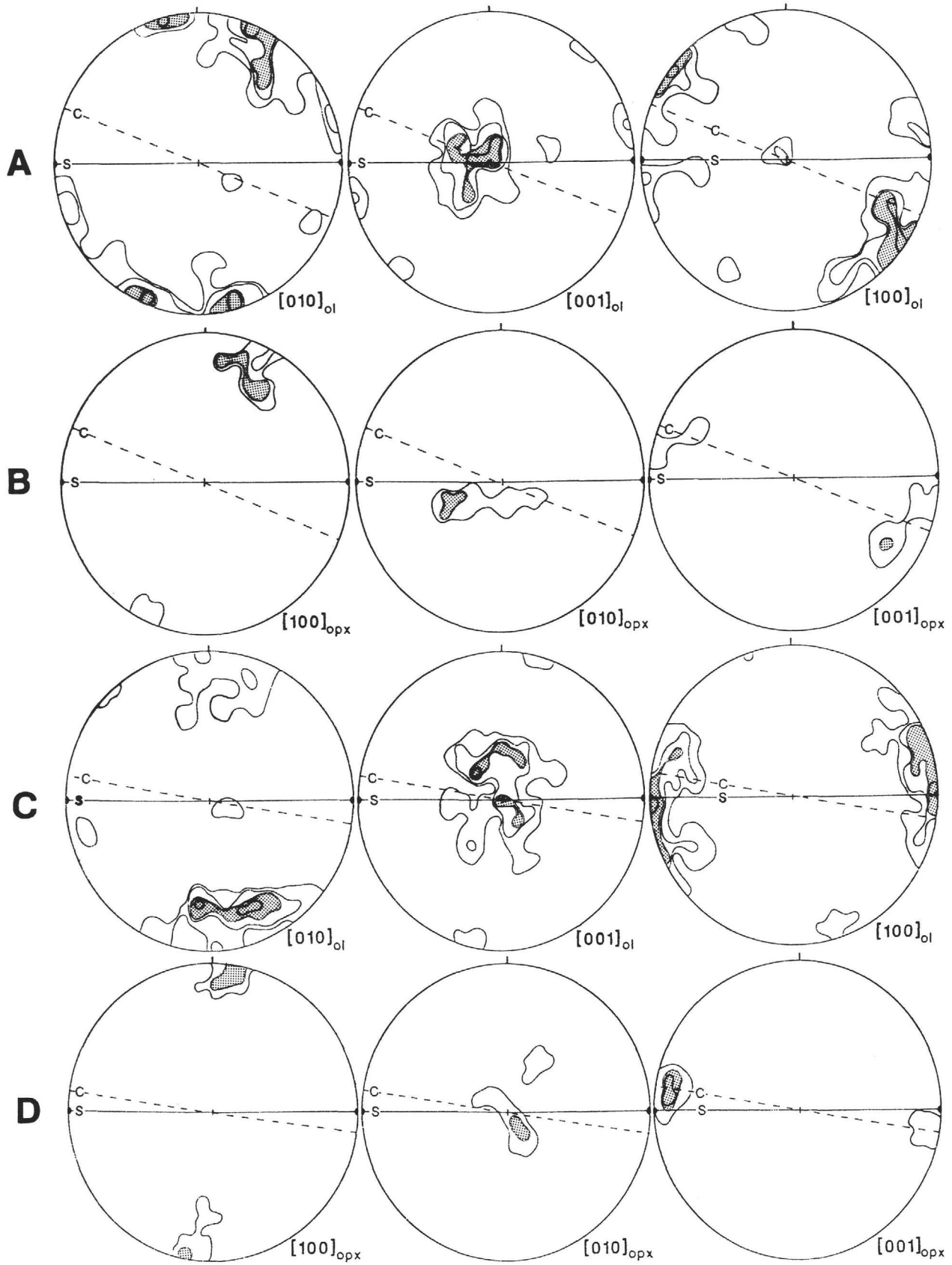


Figure 7. Olivine (A and C) and orthopyroxene (B and D) preferred orientation (equal-area projection, lower hemisphere). The solid lines represent the trace of the foliation (s) and the solid dots the attitude of the lineation; the dashed lines (c) represent the trace of the shear planes. Contours are for 18%, 13%, 8%, and 4% for olivine; 43% and 21% for orthopyroxene.

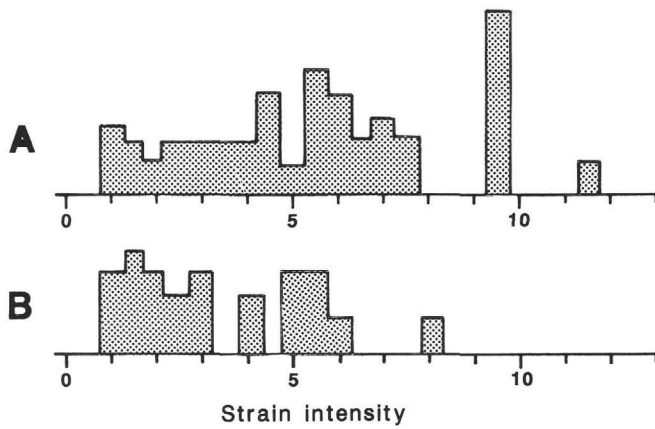


Figure 8. Strain intensity ( $\gamma$ ) determined using the formulas (A)  $\gamma = 2\cot\theta 2\alpha$  and (B)  $\gamma = \lambda_1 - \lambda_2$ , with  $\lambda_1$  and  $\lambda_2$  determined from orthopyroxene shapes.

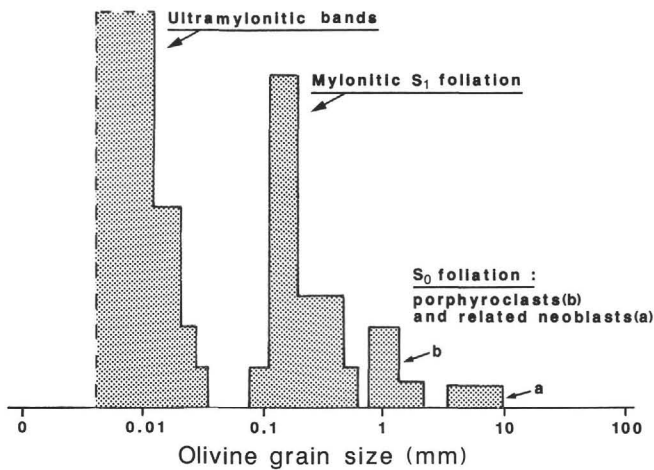


Figure 9. Variations in olivine grain size within the Hole 637A peridotites.

formation (several tens of GPa using SGR—i.e., unrealistic values—and about 180 MPa using GBM). The high stress values inferred for the mylonitization event that probably occurred at a temperature around 850°C (see next section) are consistent with that necessary to nucleate the exsolution lamellae in the orthopyroxenes by twinning or lattice inversion at this temperature ( $\approx 250$  MPa; Mercier, 1986).

#### Temperatures and Pressures of Equilibrium

Because the geochemical signature of Hole 637A peridotites is discussed in other chapters in this volume (Evans and Girardeau; Kornprobst and Tabit), we present here only the data necessary to document evolution of the equilibrium condition(s) during peridotite emplacement.

Chemical compositions of mineral phases were obtained with a CAMEBAX microprobe (Camparis Université Paris VI), using oxide standards and natural minerals (PHN 1611) for tests. The accelerating voltage was 15 kV, the beam current 40  $\mu$ A, and the counting time varied from 30 to 50 s, depending upon the elements. The olivine and spinel crystals were analyzed at their cores to best estimate their primary compositions, using normal point-analysis techniques. Because orthopyroxenes from Hole 637A peridotites are characterized by the presence of abundant exsolution lamellae, microprobe point-analysis techniques

(even with a broad beam) can not give the original composition of the pyroxene crystals. Therefore, we have integrated the exsolution lamellae composition to obtain the bulk-pyroxene original composition for the best estimate of the primary equilibrium conditions or, at least, conditions close to those existing during formation (Mercier et al., 1984). In the Hole 637A peridotites, the clinopyroxenes are much smaller than the orthopyroxenes (more than 10 times) and do not show any exsolution lamellae, as is generally observed in clinopyroxenes from mylonites. This indicates that they have been rehomogenized and/or reequilibrated during the mylonitization event.

If some degree of equilibrium was achieved during peridotite emplacement, one would expect to find correlations between certain determinant geochemical parameters tying orthopyroxene, clinopyroxene, and spinel. To test the equilibrium state, we will refer to theoretical equilibrium curves worked out using independent thermometric methods (Benoit, 1987). Figure 10 shows  $Al^*_{(opx)}$  corrected for Cr dilution effect by spinel vs. the  $Ca^*$  of pyroxenes corrected for their Na content (Mercier and Bertrand, 1984; Bertrand and Mercier, 1985). In Figure 10A ( $Al^*_{(opx)}$  vs.  $Ca^*_{(opx)}$ ), most of the data plot above the theoretical equilibrium line, which indicates that clinopyroxene is not in equilibrium with orthopyroxene, as suggested by the clinopyroxene specific texture (see preceding discussion). However, orthopyroxene records a previous equilibrium state with a clinopyroxene buffer, as the data points now fall on the  $Al^*/Ca^*$  correlation curve (Fig. 10B).

Several mineralogical thermometers or thermobarometers based on transfer reactions have been proposed to estimate the temperature and pressure of equilibrium of the studied peridotites. Using the aluminum content of coexisting orthopyroxene and spinel phases (Bertrand et al., 1987) or the diopside-transfer reaction (Benoit, 1987), the calculated equilibrium temperatures range from 970° to 1130°C for the porphyroclasts and from 730° to 970°C for the neoblasts from the shear zones (Figs. 11A and 11B). When using the En-transfer reaction of Bertrand and Mercier (1986), which is almost insensitive to the orthopyroxene composition as a result of the form of the equilibrium constant, we obtain much lower temperatures, ranging from 830° to 870°C for both porphyroclasts and neoblasts (Fig. 11C). A 0.2-GPa (Fig. 11D) maximum reequilibration pressure is inferred from the pyroxene maximum composition using the Mercier et al. (1984) barometer.

We consider that the 830°–870°C temperature and 0.2-GPa pressure reflect conditions at which the clinopyroxene recrystallized, therefore, corresponding to those at which peridotite mylonitization ended. However, this mylonitization event began at a much higher temperature ( $> 1000^\circ\text{C}$ ), as evidenced by the activation of olivine and orthopyroxene high-temperature glide systems. The 970°–1130°C temperatures are difficult to interpret; they probably reflect the prevailing conditions when the last melts were leaving the peridotite.

## DISCUSSION

During their uplift, the initially coarse-grained and locally orthopyroxene-rich peridotites cored at Hole 637A underwent two major high-temperature events:

1. Limited partial melting. These rocks suffered, at most, 6% to 9% partial melting and melt extraction (Evans and Girardeau, this volume). Traces of melt have apparently been trapped in the peridotite and crystallized into isolated interstitial crystals and irregular feldspar veins (Figs. 4A and 4B). Melting possibly started in the spinel facies (if we accept that they came from an adiabatic rising diapir; see subsequent discussion on this subject) and possibly ended at the spinel-plagioclase transition (point 1; Fig. 12). However, we cannot exclude the possibility that sig-

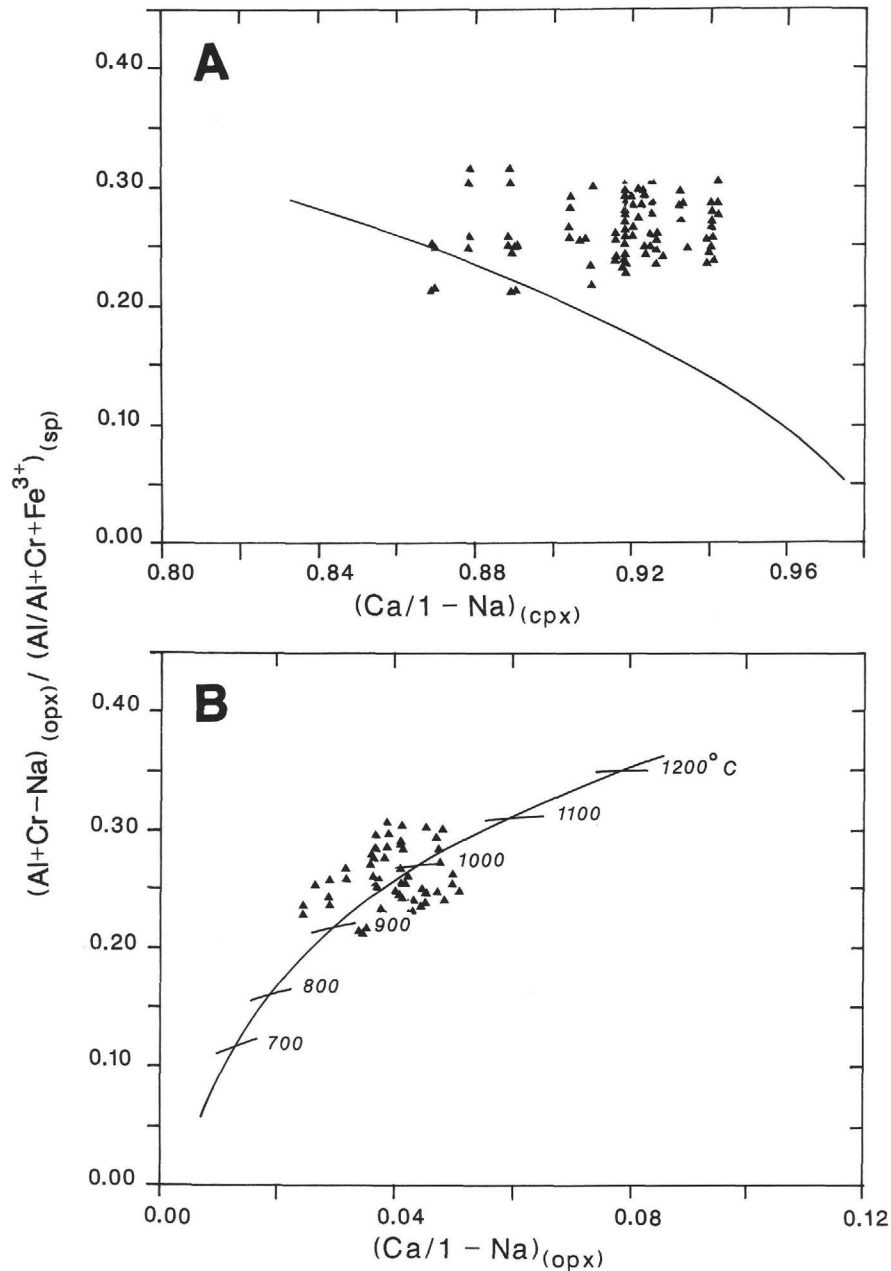


Figure 10. Correlation diagrams for pyroxenes.  $Al^*$  in orthopyroxene =  $(Al + Cr - Na)_{(opx)} / (Al/[Al + Cr + Fe^{3+}])_{(sp)}$  vs.  $Ca^*(Ca/[1 - Na])$  in (A) clinopyroxene and (B) orthopyroxene. The solid lines on both figures represent the theoretical equilibrium curves determined by Benoit (1987) using independent thermometric methods.

nificant amounts of melt existed within the peridotite until very shallow depths to account for the low temperature (1100°–970°C) of equilibrium recorded by the primary phases. On the other hand, the melt extraction possibly ended with the beginning of the peridotite stretching, as suggested by the textural relationships between plagioclase crystallization and mylonitic foliation development.

2. High strain-stress stretching event. This deformation began at high temperature (above 1000°C) (point 2; Fig. 12) and probably ended at 850°C (point 3; Fig. 12) at very shallow depth (<7 km). Deformation occurred by plastic flow in a simple shear regime, under high strain ( $\gamma \approx 12$ ) and stress (180 MPa) conditions, inducing the development of a penetrative  $S_1$

mylonitic foliation that is locally crosscut by ultramylonitic bands. High-temperature (800°–900°C) amphiboles developed in static conditions just after the peridotite mylonitization (Agrinier et al., this volume). This suggests that mylonitization of the peridotite occurred in hydrous conditions, which would explain the relatively low recrystallization temperatures for the clinopyroxene.

After these two major high-temperature metamorphic events, the peridotite underwent some hydrothermal alteration, which probably began at high temperature (point 4; Fig. 12). Then it was intensively serpentinized at a temperature below 300°C (point 5; Fig. 12) (Agrinier et al., this volume). This alteration oc-

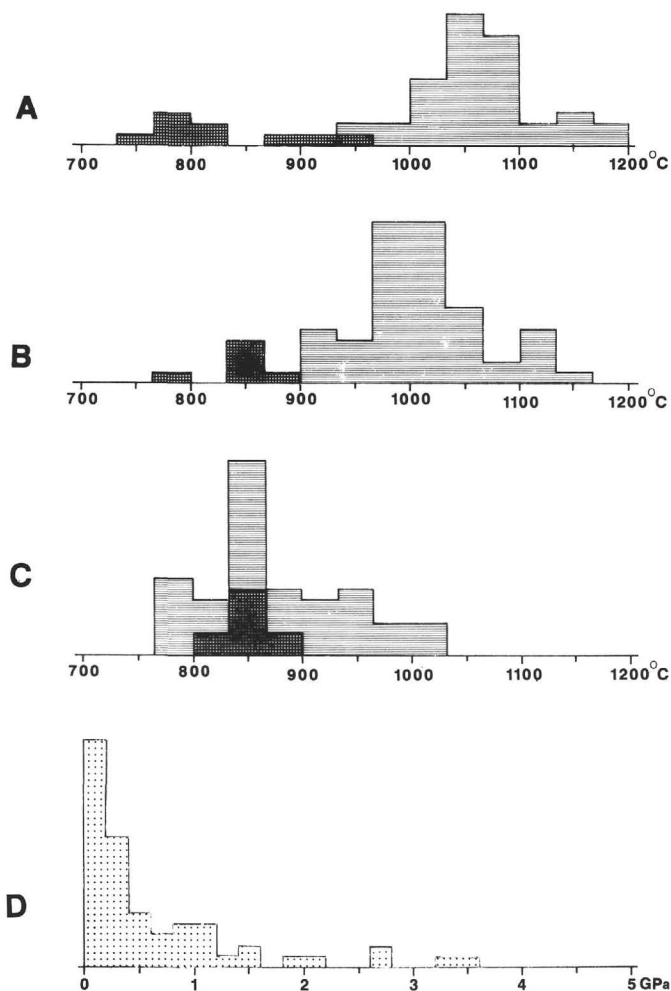


Figure 11. Calculated temperatures and pressures for the Hole 637A peridotites. The horizontal strips on the histograms are for porphyroclasts and the vertical ones are for the recrystallized grains from the shear zones. **A.** Orthopyroxene-spinel thermometer; Bertrand et al. (1987) and Mercier et al., 1987. **B.** Diabase-transfer thermometer; Benoit et al. (1987). **C.** Enstatite-transfer thermometer; Bertrand et al. (1985). **D.** Empirical two-pyroxene barometer; Mercier et al. (1984).

curred in static conditions and probably after the final emplacement of the peridotite in its present position. During its ascent, the peridotite probably underwent some lower temperature ductile deformation, which was overprinted by later alterations and is not observed in the studied samples.

The Hole 637A peridotites display a homogeneous  $S_1$  foliation crosscut by thin, ultramytonitic shear bands. Both dip  $30^\circ$  on average in the upper 50 m drilled, increasing up to  $70^\circ$  down-section. The lineation maintains a constant attitude throughout the cored section; it is mostly oriented downdip in the foliation except in a few places where it is at about  $45^\circ$  from the downdip line. The foliation in the peridotite appears to dip to the east or east-northeast (see "Site 637" chapter; Shipboard Scientific Party, 1987; Boillot et al., 1986b, 1987). The plane along which shearing occurred had a northeast normal component of movement with a local north-northeast strike-slip component. The overall attitudes of both foliation and lineation are not compatible with transform fault displacement, which makes it unlikely that these rocks were emplaced in a transcurrent zone.

### ORIGIN OF THE HOLE 637A PERIDOTITES

Assuming that the Hole 637A peridotites were emplaced during continental rifting, one can formulate two hypotheses for

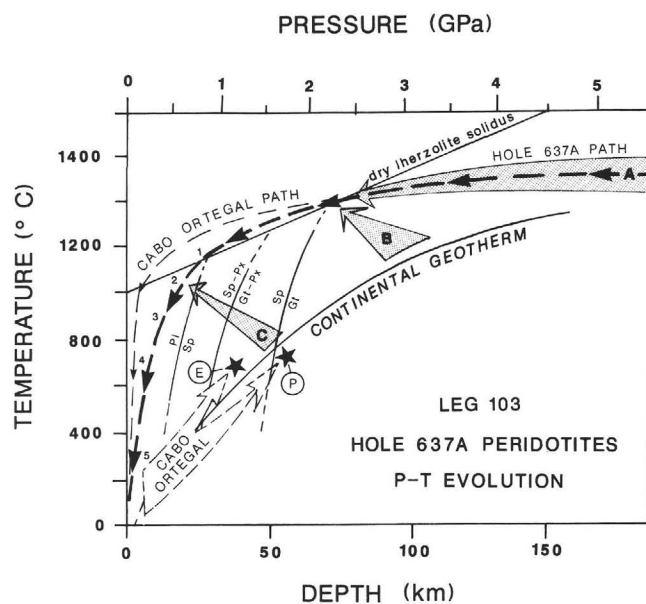


Figure 12. Pressure-temperature evolution of the peridotites drilled at Hole 637A. **A** = adiabatic rising mantle path (Nicolas, 1986); **B** and **C** = reheated lithosphere paths; **1** = possible end of melting; **2** = field of beginning of mylonitization of the peridotite; **3** = end of mylonitization; **4** = field of beginning of hydrothermal alteration; **5** = field of intensive serpentinization; **Gt** = garnet; **Sp** = spinel; **Pl** = plagioclase; **Px** = pyroxene; **E** and **P** = eclogites and peridotites from Cabo Ortégual Massif (Galicia, Spain).

origin: (1) the peridotites represent a piece of the lithospheric subcontinental mantle of the Iberian plate or (2) the peridotites represent asthenospheric material accreted to the lithosphere during rifting. Any answer must account for the fact that the peridotite underwent a small amount of partial melting during its uplift, followed by an extremely strong deformation under very high-stress conditions, high but decreasing temperature ( $1000^\circ$  to  $860^\circ\text{C}$ ), and probably at very shallow depth ( $< 7$  km).

Considering realistic geothermal gradients (Mercier and Carter, 1975; Allègre and Bottinga, 1974; Mercier, 1980; Sclater et al., 1980; Bertrand et al., 1986) and the temperature and pressure of melting estimated for the Hole 637A peridotites, we conclude that this melting could not have occurred within either passive continental mantle or passive oceanic mantle lithosphere but only beneath a tectonically active domain where the isotherm pattern is perturbed by the rise of hot asthenospheric material close to the surface. Beneath areas with high thermal gradients, such as steady-state spreading ridges, heat loss by conduction in ascending hot material passing through the lithosphere is significant even at great depth. This has been shown by theoretical modeling, which indicates that the adiabatic regime is perturbed at a depth of about 26 km for rising velocities below 1 cm/yr (Bottinga and Allègre, 1973; Allègre and Bottinga, 1974). Hence, at shallow levels, it appears quite impossible for subcrustal peridotites to be heated sufficiently to melt (path C; Fig. 12). Because the cooling effect is particularly large beneath stretched continental lithosphere (Alvarez et al., 1984), we consider that the partial melting of the Hole 637A peridotites occurred within some asthenospheric rising material (path A; Fig. 12) and that they were accreted later to the lithosphere. Kornprobst and Tabit (this volume) suggest that this asthenospheric material initially represents some subcontinental material that has been reheated at great depths (path B; Fig. 12).

The peridotite has not undergone a large melting event, but only limited melt extraction, which probably ended at the spinel/plagioclase boundary (Evans and Girardeau, this volume),

indicating that adiabatic conditions were not achieved at depth during the peridotite ascent (point 1; Fig. 12). This can reflect a very cold thermal regime for the lithosphere through which the hot mantle was rising or very low rising velocities. Both possibilities are consistent conditions for a rift environment (Boudier and Nicolas, 1985).

We have observed that the dip of the mylonitic shear planes for the Hole 637A peridotites varies from 30° to 70° to the east or east-northeast, that the shear directions trend east or east-northeast, and that the shear sense is normal (with a local strike-slip component) along the shear plane. These geometric and kinetic data are compatible with those expected at the edge of a rising asthenospheric dome. Because the mylonitic structures result from high-strain-high-stress deformations, we suggest that they formed when the asthenospheric material arrived near the surface, where steep thermal gradients are expected between the ascending material and the surrounding lithosphere. Such conditions are expected in a rift environment (Mercier, 1977; Boudier and Nicolas, 1985) or where the stretched lithosphere has just reached the oceanic accretion stage.

The foliation and lineation attitudes are also compatible with those formed by displacement along a gently dipping normal fault, as proposed by Boillot et al. (1986a, 1987). But in this case, the fault would have to pass at the edge of or through an asthenospheric dome to account for the physical conditions prevailing during the melting and subsequent shearing of the Hole 637A peridotites.

## CONCLUSIONS

The structural and microstructural data presented in this study support the continental rift origin already proposed for the Hole 637A peridotites using petrochemical arguments (Boillot et al., 1980). This study has shown that the Hole 637A peridotites were probably asthenospheric material that rose adiabatically within the lithosphere. Upon arrival near the surface, this material underwent a high-strain-high-stress mylonitization event (i.e., in lithospheric conditions), and the geometry and kinematics of the mylonitization phase are consistent with a roughly east-west opening of the Atlantic Ocean. After emplacement in its present position, the peridotite was strongly serpentinized and fractured.

## ACKNOWLEDGMENTS

The authors thank J.-C. C. Mercier, V. Benoit, N. Ben Jamaa, and G. Dubuisson for helpful discussions during the study of these samples. We also thank J.-C. C. Mercier, H. Avé Lallemand, N. L. Carter, A. W. Meyer, and G. Boillot for reviewing the manuscript. We wish to extend our thanks to G. Girardeau, who typed the manuscript. This work was supported by ATP GGO. This is IGP contribution no. 1026; UA 1093.

## REFERENCES

- Allègre, C. J., and Bottinga, Y., 1974. Tholeiite, alkali basalts and ascent velocity. *Nature*, 252:31-32.
- Alvarez, F., Virieux, J., and Le Pichon, X., 1984. Thermal consequences of lithosphere extension over continental margins: the initial stretching phase. *Geophys. J. R. Astron. Soc.*, 78:389-411.
- Aumento, F., and Loubat, H., 1971. The Mid-Atlantic Ridge near 46°S: serpentinized ultramafic intrusions. *Can. J. Earth Sci.*, 18:631-664.
- Benoit, V., 1987. Etat d'équilibre des péridotites du manteau supérieur: méthodes et applications au plateau du Colorado [Ph.D. thesis]. IGP Paris et Université Paris VII.
- Bertrand, P., and Mercier, J.-C. C., 1985. The mutual solubility of coexisting clino- and orthopyroxene: toward an absolute geothermometer for the natural system. *Earth Planet. Sci. Lett.*, 76:109-122.
- Bertrand, P., Sotin, C., Gaulier, J.-M., and Mercier, J.-C. C., 1987. La solubilité de l'aluminium dans l'orthopyroxène: inversion globale des données expérimentales du système chimique MgO-Al<sub>2</sub>O<sub>3</sub>-SiO<sub>2</sub>. *Bull. Soc. Geol. Fr.*, 29:821-832.
- Bertrand, P., Sotin, C., Mercier, J.-C. C., and Takahashi, E., 1986. From the simplest chemical system to the natural one: garnet, peridotite barometry. *Contrib. Mineral. Petrol.*, 93:168-178.
- Beslier, M.-O., Girardeau, J., and Boillot, G., 1988. Lithologie et structure des péridotites à plagioclase bordant la marge continentale passive de la Galice (Espagne). *C. R. Acad. Sci. Ser. 2*, 306:373-380.
- Boillot, G., Auxiètre, J. L., Dunand, J. P., Dupeuble, P. A., and Mauffret, A., 1979. The northern Iberian margin: a Cretaceous passive margin deformed during Eocene. In Talwani, M., Hay, W., and Ryan, W.B.F. (Eds.), *Deep Drilling Results in the Atlantic Ocean: Continental Margins and Paleoenvironment*: Am. Geophys. Union, Maurice Ewing Ser., 3:138-153.
- Boillot, G., Comas, M., Girardeau, J., Kornprobst, J., Loreau, J.-P., Malod, J., Mougénot, D., and Moullade, M., 1986a. Fonds sous-marins basaltiques et ultramafiques au pied d'une marge stable. Résultats préliminaires de la campagne Galinaute (plongées du submersible *Nautille* à l'ouest de l'Espagne) *C. R. Acad. Sci. Ser. 2*, 303:1719-1724.
- \_\_\_\_\_, 1986b. Amincissement de la croûte continentale et dénudation tectonique du manteau supérieur sous les marges stables: à la recherche d'un modèle—l'exemple de la marge continentale de la Galice. *Bull. Cent. Rech. Explor. Prod. Elf Aquitaine*, 10:95-104.
- Boillot, G., Grimaud, S., Mauffret, A., Mougénot, D., Kornprobst, J., Mergoil-Daniel, J., and Torrent, G., 1980. Ocean-continent boundary off the Iberian margin: a serpentinite diapir west of the Galicia Bank. *Earth Planet. Sci. Lett.*, 48:23-34.
- Boillot, G., Recq, M., Winterer, E. L., Meyer, A. W., Applegate, J., Baltuck, M., Bergen, J. A., Comas, M. C., Davies, T. A., Dunham, K., Evans, C. A., Girardeau, J., Goldberg, D. G., Haggerty, J., Jansa, L. F., Johnson, J. A., Kasahara, J., Loreau, L.-P., Luna-Sierra, E., Moullade, M., Ogg, J., Sarti, M., Thuro, J., and Williamson, M., 1987. Tectonic denudation of the upper mantle along passive margins: a model based on drilling results (ODP Leg 103, western Galicia margin, Spain). *Tectonophysics*, 132:335-342.
- Bonatti, E., and Hamlyn, P. R., 1978. Mantle uplifted block in the western Indian ocean. *Science*, 201:249-251.
- \_\_\_\_\_, 1981. Oceanic rocks. In Emiliani, C. (Ed.), *The Sea* (Vol. 7): New York (Wiley), 241-283.
- Bonatti, E., Hamlyn, R. E., and Ottonello, G., 1981. The upper mantle beneath a young oceanic rift: peridotites from the Island of Zabargad (Red Sea). *Geology*, 9:474-479.
- Bonatti, E., and Honnorez, J., 1976. Sections of Earth's crust in the equatorial Atlantic. *J. Geophys. Res.*, 81:4104-4116.
- Bonatti, E., Ottonello, G., and Hamlyn, R. E., 1986. Peridotites of the Island of Zabargad (St. John), Red Sea: petrology and geochemistry. *J. Geophys. Res.*, 91:599-631.
- Bottinga, Y., and Allègre, C. J., 1973. Thermal aspect of sea floor spreading and the nature of the oceanic crust. *Tectonophysics*, 18:1-17.
- Boudier, P., 1979. Microstructural study of three peridotite samples drilled at the western margin of the Mid-Atlantic Ridge. In Melson, W. G., and Rabinowitz, P. D., et al., *Init. Repts. DSDP*, 45: Washington (U.S. Govt. Printing Office), 603-608.
- Boudier, F., and Nicolas, A., 1985. Harzburgite and lherzolite subtypes in ophiolitic and oceanic environments. *Earth Planet. Sci. Lett.*, 76:84-92.
- Bryan, W. B., Juteau, T., Adamson, A. C., Autio, A.L.K., Becker, K., Mansour Bina, M., Eissen, J.-P., Toshitsugu, F., Grove, T. L., Hamano, Y., Hebert, R., Komor, S. K., Kopietz, J., Krammer, K., Loubet, M., Moos, D., and Richards, H. G., 1986. Coring the crust and mantle. *Nature*, 323:492-493.
- Brun, J. P., and Burg, J. P., 1982. Combined thrusting and wrenching in the Ibero-Armorican arc: a corner effect during continental collision? *Earth Planet. Sci. Lett.*, 61:319-332.
- Burg, J. P., 1981. Tectonique tangentielle hercynienne en Vendée littorale: signification des linéations E-W dans les porphyroïdes à foliation horizontale. *C. R. Acad. Sci. Ser. 2*, 293:849-854.
- Burg, J. P., Balé, P., Brun, J. P., and Girardeau, J., 1987. Stretching lineation and transport direction in the Ibero-Armorican arc during the Siluro-Devonian collision. *Geodyn. Acta*, 1:71-87.
- Burg, J. P., Iglesias, P., Laurent, P., Matte, P., and Ribeiro, A., 1981. Variscan intracontinental deformation: the Porto-Tomar-Cordoba shear zone (SW Iberian Peninsula). *Tectonophysics*, 78:161-177.
- Carter, N., and Avé Lallemand, H. G., 1970. High temperature flow of dunite and peridotite. *Geol. Soc. Am. Bull.*, 81:2181-2182.

- Darot, M., and Boudier, F., 1975. Mineral lineation in deformed peridotites kinematic meaning. *Petrologie*, 1:226-236.
- Decandia, F. A., and Elter, P., 1982. La "zona" ophiolitifera del Braccione nel settore compreso fra Lavanto e la Val Graveglia (Apennino Ligure). *Proc. Congr. Geol. Soc. Ital.*, 66:37-64.
- Dubuisson, G., Girardeau, J., and Mercier, J.-C.C., 1987. Petrology of the Limousin ophiolite (western French Massif Central): implication for the Variscan orogeny. *Terra Cognita*, 7:176.
- Girardeau, J., Dubuisson, G., and Mercier, J.-C.C., 1986. Cinématique de mise en place des ophiolites et nappes cristallines du Limousin: ouest du Massif Central français. *Bull. Soc. Geol. Fr.*, 28:849-860.
- Groupe Galice, 1979. The continental margin off Galicia and Portugal: acoustical stratigraphy, dredge stratigraphy and structural evolution. In Sibuet, J.-C., and Ryan, W.B.F., et al., *Init. Repts. DSDP*, 47, Pt. 2: Washington (U.S. Govt. Printing Office), 633-662.
- Helmstaedt, H., 1977. Postmagmatic textures and fabrics of gabbros and peridotites from DSDP Site 334. In Aumento, F., and Melson, W. G., et al., *Init. Repts. DSDP*, 37: Washington (U.S. Govt. Printing Office), 767-762.
- Ibarguchi Gil, I., Ben Jamaa, N., Girardeau, J., Mercier, J.-C.C., and Agrinier, P., 1987. The ophiolite sequence of the Cabo Ortégala complex (NW Spain): MORB-type mafic rocks and websterite rich peridotites. *Terra Cognita*, 7:176.
- Iglesias, M., Ribeiro, M. L., and Ribeiro, A., 1983. La interpretación aloctonista de la estructura del noroeste Peninsular. In Ries, J. R., (Ed.), *Geología de España* (Vol. 1): I.G.M.E., 459-467.
- Kastens, K., Mascle, J., Aurooux, C. A., Bonatti, E., Broglia, C., Chanel, J., Curzi, P., Emeis, K. C., Glagon, C., Hasegawa, S., Hieke, W., Mascle, G., McCoy, F., McKenzie, J., Nendelions, I., Müller, C., Rehault, J.-P., Robertson, A., Sartori, R., Sprovieri, R., and Torri, N., 1986. La campagne 107 du JOIDES Resolution (Ocean Drilling Program) en Mer Tyrrhénienne: premiers résultats. *C. R. Acad. Sci. Ser. 2*, 303:391-396.
- Kornprobst, J., and Vielzeuf, D., 1984. Transcurrent crustal thinning: a mechanism for the uplift of deep continental crust/upper mantle associations. In Kornprobst, J. (Ed.), *Kimberlites*: Amsterdam (Elsevier), 347-359.
- Lagabrielle, Y., 1982. Ophiolite et croûte océanique: tectonique et environnement sédimentaire [Thesis]. Univ. Brest.
- Lallemand, S., Mazé, J. P., Monti, S., and Sibuet, J.-C., 1986. Présentation d'une carte bathymétrique de l'Atlantique nord-est. *C. R. Acad. Sci. Ser. 2*, 300:145-149.
- Lefort, J. P., 1980. Un "fit" structural de l'Atlantique Nord, arguments géologiques pour corrélérer les marqueurs géophysiques reconnus sur les deux marges. *Mar. Geol.*, 37:366-369.
- Lefort, J. P., and Ribeiro, A., 1980. La faille Porto-Badajoz-Cordoue a-t-elle contrôlé l'évolution de l'océan paléozoïque sud-armoricain? *Bull. Soc. Geol. Fr.*, 22:465-462.
- Lemoine, M., Tricart, P., and Boillot, G., 1987. Ultramafic and gabbroic ocean floor of the Ligurian Tethys (Alps, Corsica, Apennines): in search of a genetic model. *Geology*, 16:62-65.
- Lombardo, H., and Pognante, U., 1982. Tectonic implications in the evolution of the Western Alps ophiolites metagabbros. *Ophioliti*, 7: 371-394.
- Matte, P., 1983. Two geotraverses across the Ibero-Armorican Variscan arc of western Europe. In Rast, W., and Delany, M. (Ed.), *Profiles of Orogenic Belts*: Washington (Am. Geophys. Union), 53-81.
- \_\_\_\_\_, 1986. Tectonics and plate tectonics models for Variscan belts in Europe. *Tectonophysics*, 126:329-374.
- Mercier, J.-C.C., 1977. Natural peridotites: chemical and rheological heterogeneity of the upper mantle [Ph.D. thesis]. Univ. of New York, Stony Brook.
- \_\_\_\_\_, 1980. Single-pyroxene thermobarometry. *Tectonophysics*, 70: 1-37.
- \_\_\_\_\_, 1986. Olivine and pyroxene. In Wenk, H. R. (Ed.), *Preferred Orientation in Deformed Metals: An Introduction to Modern Texture Analysis*: New York (Academic Press), 407-430.
- Mercier, J.-C.C., Anderson, D. A., and Carter, N., 1977. Stress in the lithosphere: inference from steady state flow of rocks. *Pure Appl. Geophys.*, 115:129-226.
- Mercier, J.-C.C., Benoit, V., and Girardeau, J., 1984. Equilibrium state of diopside-bearing harzburgites from ophiolites: geobarometric and geodynamic implications. *Contrib. Mineral. Petrol.*, 86:391-403.
- Mercier, J.-C.C., and Bertrand, P., 1984. Thermobarométrie pyroxénique: quelques méthodes basées sur des réactions de transfert. In Gabis, V., and Lagache, M. (Eds.), *Thermobarométrie et Barométrie Géologique*: Paris (Soc. Fr. Mineral. Cristallogr.), 237-280.
- Mercier, J.-C.C., and Carter, N. L., 1975. Pyroxene geotherms. *J. Geophys. Res.*, 80:3349-3362.
- Michael, P. J., and Bonatti, E., 1985. Petrology of ultramafic rocks from Sites 556, 558, and 560 in the North Atlantic. In Bougault, H., Cande, S. C., et al., *Init. Repts. DSDP*, 82: Washington (U.S. Govt. Printing Office), 523-528.
- Montadert, L., de Charpal, O., Roberts, D., Guennoc, P., and Sibuet, J.-C., 1979. Northeast Atlantic passive margin: rifting and subsidence processes. In Talwani, M., Hay, W., Ryan, W.B.F. (Eds.), *Deep Drilling Results in the Atlantic Ocean: Continental Margins and Paleoenvironments*: Am. Geophys. Union, Maurice Ewing Ser., 3:154-186.
- Montadert, L., Winnock, E., Delteil, J. R., and Grau, G., 1974. Continental margins of Galicia-Portugal and Bay of Biscay. In Burk, C. A., and Drake, C. L. (Eds.), *The Geology of Continental Margins*: Berlin (Springer-Verlag), 323-342.
- Nicholls, I. D., Ferguson, J., Jones, H., Marks, G. P., and Nutter, J. C., 1981. Ultramafic rocks from the ocean floor southwest of Australia. *Earth Planet. Sci. Lett.*, 56:362-374.
- Nicolas, A., 1984. Lherzolites of the western Alps: a structural review. In Kornprobst, J. (Ed.), *Kimberlites II: The Mantle and Crust-Mantle Relationships*: Amsterdam (Elsevier), 333-345.
- \_\_\_\_\_, 1986. A melt extraction model based on structural studies on mantle peridotites. *J. Petrol.*, 27:99-102.
- Nicolas, A., Boudier, F., Lyberis, N., Montigny, R., and Guennoc, P., 1985. Zabargad (St. John) Island: a key-witness of early rifting in the Red Sea. *C. R. Acad. Sci. Ser. 2*, 301:1063-1068.
- Nicolas, A., Boudier, F., and Montigny, R., 1987. Structure of Zabargad Island and early rifting of the Red Sea. *J. Geophys. Res.*, 92: 461-474.
- Nicolas, A., and Poirier, J.-P. (Eds.), 1976. *Crystalline Plasticity and Solid State Flow in Metamorphic Rocks*: London (Wiley).
- Obata, M., 1977. Petrology and petrogenesis of the Ronda high-temperature peridotite intrusion, southern Spain [Ph.D. thesis]. Massachusetts Inst. Technology.
- Post, R., 1973. The flow of Mt. Burnet dunite [Ph.D. thesis]. Univ. of California, Los Angeles.
- Ramsay, J. G. (Ed.), 1967. *Folding and Fracturing of Rocks*: London (McGraw-Hill).
- Ross, J. V., Avé Lallemant, H. G., and Carter, N., 1980. Stress dependence of recrystallized grain and subgrain size in olivine. *Tectonophysics*, 70:39-61.
- Sclater, J. G., Jaupart, C., and Galson, D., 1980. The heat flow through oceanic and continental crust and the heat loss of the earth. *Rev. Geophys. Space Phys.*, 18:269-311.
- Shipboard Scientific Party, 1987. Site 637. In Boillot, G., Winterer, E. L., et al., *Proc. ODP, Init. Repts.*, 103: College Station, TX (Ocean Drilling Program), 123-219.
- Sibuet, J.-C., Mazé, J.-P., Amortila, P., and Le Pichon, X., 1987. Physiography and structure of the western Iberian continental margin off Galicia, from Sea Beam and seismic data. In Boillot, G., Winterer, E. L., et al., *Proc. ODP, Init. Repts.*, 103: College Station, TX (Ocean Drilling Program), 77-97.
- Sibuet, J.-C., and Ryan, W.B.F., 1979. Site 398: evolution of the west Iberian passive continental margin in the framework of the early evolution of the North Atlantic Ocean. In Sibuet, J.-C., Ryan, W.B.F., et al., *Init. Repts. DSDP*, 47, Pt. 2: Washington (U.S. Govt. Printing Office), 761-776.
- Sigurdsson, H., 1977. Spinels in Leg 37 basalts and peridotites: phase chemistry and zoning. In Aumento, F., and Melson, W. G., et al., *Init. Repts. DSDP*, 37: Washington (U.S. Govt. Printing Office), 883-890.
- Sinton, J. M., 1979. Petrology of Alpine-type peridotites from Site 395, DSDP, Leg 45. In Melson, W. G., and Rabinowitz, P. D., et al., *Init. Repts. DSDP*, 45: Washington (U.S. Govt. Printing Office), 595-601.
- Styles, P., and Gerdes, K. D., 1983. St. John Island (Red Sea): a new geophysical model and its implications for the emplacement of ultramafic rocks in fracture zone and at continental margin. *Earth Planet. Sci. Lett.*, 66:353-368.
- Tiezzi, L. J., and Scott, R. B., 1980. Crystal fractionation in a cumulate gabbro, Mid-Atlantic Ridge, 26°N latitude. *J. Geophys. Res.*, 85(B10):5438-5454.

- Tubia, S. M., and Cuevas, J., 1977. Structure et cinématique liée à la mise en place des péridotites de Ronda (Cordillères Bétiques, Espagne). *Geodin. Acta*, 1:59-69.
- Van Calsteren, P.W.C., 1978. Geochemistry of the polymetamorphic mafic-ultramafic complex at Cabo Ortégal (NW Spain). *Lithos*, 11: 61-72.
- Vielzeuf, D., and Kornprobst, J., 1984. Crustal splitting and the emplacement of Pyrenean lherzolites and granulites. *Earth Planet. Sci. Lett.*, 67:87-96.

Vögel, D. E., 1967. Petrology of an eclogite and pyrigarnite bearing polymetamorphic rock complex at Cabo Ortégal, NW Spain. *Leidse Geol. Meded.*, 40:121-213.

**Date of initial receipt: 23 March 1987**

**Date of acceptance: 13 January 1988**

**Ms 103B-135**